CONVECTIVE DISCRETIZATION DEPENDENCE ON THE PERFORMANCE OF SEVERAL TURBULENCE MODELS FOR AIRFOIL STALL FLOW

Kobayashi, M.H., Marques, N.P.C., Pereira, J.C.F.
Instituto Superior Técnico
Mechanical Engineering Department

Abstract

Numerical calculation of time averaged Navier-Stokes equations are reported for the flow around an high-lift aerofoil at Re = $2x10^6$, Ma = 0.15 and an angle of attack of 13.3°. A comparison is made with experimental results. Three numerical schemes have been used for convection discretization and for each numerical scheme four turbulence models, standard k-ε, Huang and Coakley's k-ε, Menter's SST and Gibson and Launder's RST, were used to close the time averaged Navier-Stokes equations. Calculations obtained in a 352x64 mesh show that the numerical scheme may influence the calculations in this specific case, in a rather unusual manner via a stronger coupling with the turbulence model. The performance of the turbulence models when used with the same numerical scheme show the superiority of the two-layer RST model over two-equation models.

Introduction

The calculation of turbulent shear flows in Aeronautics is one of the challenging tasks yet to be mastered up to a level where one can make systematic, consistent and accurate predictions of the flow fields involved. The present study concentrates itself on the case of an incipient separation that precedes stall. The configuration to be presented is Aerospatiale's A-Airfoil, for which detailed measurements were taken by Piccin and Cassoudesalle[1]. This aerofoil is a high lift one, and the measurements were taken for a mach number of 0.15, a Reynolds number of $2.0x10^6$ (based on chord), an angle of attack of 13.3° and a chord of 0.6 meters. To remove the transition problem, this was fixed at 12 percent of chord, for the suction side of the aerofoil, and at 30 percent of chord for the pressure side.

This flowfield configuration is characterized by the separation that occurs at the trailing edge, due to the value of the angle of attack and Reynolds number. This separation will be the main reason for the levels of C_L and C_D that the profile will have. The zone of dead air that exists at the trailing edge severely affects the pressure values in that region and, by consequence, the total lift and drag. This entire process in a phenomena of a deeply viscous character, and therefore out of reach for conventional prediction methods based on inviscid theory.

Our main goal in the present work is to compare the performance of a second-order differential Reynolds stress turbulence model solution with two-equation models without neglecting the influence of the numerical discretization scheme to the solution error. For the range of high-Reynolds numbers involved, the discretization of the convective flux becomes of critical importance (specially in conjunction with second order turbulence models where it can indeed impair convergence of the numerical method[2]). So, for the discretization of the convective flux three non-oscillatory high order methods have been selected, namely, MINMOD, MUSCL[3] and SONIC-Q[4].

Numerical Scheme

Numerical computations have been carried out using the primitive variable formulation in a finite-volume pressure-correction framework and with a collocated mesh arrangement (see [5] for details).

Consider a 1D uniform grid with cell parameter, h, covering without superposition the domain of interest (the extension of the techniques for multidimensional problems and for non-uniform grids is straightforward and is omitted for clarity). Denote the interfaces quantities by the indices, i, and the cell center, where the variables are stored, by half the adjacent indices. With this convention the problem at hand is to interpolate the value of the variables, represented generically by ϕ, at the interfaces. In this work these values are computed using the following upstream interpolation practice:

$$\phi_i = a^+ \phi_i^+ + a^- \phi_i^-$$

where

$$a^{\pm} = \left(\frac{u_l \pm |u_l|}{2u_l} \right)_i$$

and the values of $(u_l)_i$ relative to the mass flux are obtained by using PWIM interpolation. The values of $\phi_i^{\pm}$ are calculated by a linear reconstruction of the form:

$$L_j(x;\phi) = \phi_j + S_j(x - x_j) \qquad (2.1)$$

for $|x-x_j| \le \frac{h}{2}$, and j = i-1/2, i+1/2.

Then,

$$\phi_i^{\pm} = L_{i\pm 1/2}(x_i^{\pm};\phi)$$

So the interpolation problem has been reduced to the evaluation of the slope S_j in Eq. (2.1).

MINMOD Scheme

Denote,

$$s_j = \frac{\phi_{j+1/2} - \phi_{j-1/2}}{h}, \; j = i,\ i+1$$

then, in the MINMOD scheme S_j at the cell center is computed by,

$$S_j^{MM} = \text{minmod}\,(s_{j+1/2},\ s_{j-1/2}),\ j = i - 1/2,\ i + 1/2$$

where, given two real numbers x and y, the minmod function is defined as,

$$\text{minmod}(x,y) = \begin{cases} min(|x|,|y|), & \text{if } xy > 0 \\ 0, & \text{otherwise} \end{cases}$$

MUSCL Scheme

This scheme evaluates S_j at the cell center by,

$$S_j^{VL} = \text{minmod}\left(\frac{s_{j-1/2} + s_{j+1/2}}{2}, 2S_j^{MM}\right),$$
$$j = i - 1/2,\ i + 1/2$$

Both the MINMOD and the Van Leer schemes are second order accurate (in the L_1 norm) and TVD. However, it is well known that all TVD schemes, no matter how they are construct, must lose accuracy at local extrema[6]. To circumvent this loss of accuracy Harten and Osher[7] have introduced a new class of uniformly second order accurate, e.g. the UNO2 scheme, which unlike TVD schemes are not required to damp the values at local actual extremum, but is only required to diminish (non-increase) the number of them. More recently the "compressibility" of this scheme has been enhanced by Huynh[8], who introduced the class of SONIC schemes. Next we present the SONIC-Q scheme proposed by the authors and which belong to this class.

SONIC—Q scheme

In this scheme we take advantage of the data in the slope and curvature computations to increase the accuracy in the smooth regions of the flow (bulk portion of the domain), i.e.,

$$S_j^{SONIC-Q} = \text{minmod}\left[2\left(\phi_{j+1/2}^{Q} - \phi_j\right), \text{sgn}\left(S_j^{UNO2}\right)\max\left(\left|2S_j^{MM}\right|, \left|S_j^{UNO2}\right|\right)\right],$$

for $j = i - 1/2, i + 1/2$

where ϕ_i^Q is the value at interface obtained using QUICK[9] scheme and the slope, S_j^{UNO2} is computed as follows: let c_j denote,

$$c_j = \frac{s_{j+1/2} - s_{j-1/12}}{2h} = \frac{\phi_{j+1} - 2\phi_j + \phi_{j-1}}{2h^2},$$
$$j = i - 1/2, i + 1/2$$

Define c_i in the interfaces by,

$$c_i = \text{minmod}(c_{i-1/2}, c_{i+1/2})$$

Denote by, t_j, the second order accurate approximation to the slope at the cell center,

$$t_j^{\pm} = s_{j\pm 1/2} \mp c_{j\pm 1/2}h,\ j = i - 1/2, i + 1/2$$

The slope S_j^{UNO2} is finally computed from $t_j^{\pm}$ by,

$$S_j^{UNO2} = \text{minmod}\left(t_j^+, t_j^-\right),\ j = i - 1/2, i + 1/2$$

The non-oscillatory behavior and high accuracy of SONIC-Q follow from the definition of the SONIC class.

Turbulence Models

The turbulence models employed in this study were of two types: Two-Equation models (Standard k-ε model of Jones and Launder[10] (JL), Low-Reynolds k-ε model of Huang and Coakley[11], HC, and the k-ε/k-ω model of Menter[12], SST); Reynolds Stress Transport Model of Gibson and Launder[13] (RST), 1978, using the set of constants proposed by Craft and Launder[14]. In addition, a truncated form of the wall reflection part of the pressure strain model was used, as suggested by Lien and Leschziner[2]. As the standard form of this model is adequate for a high Reynolds situation, the above mentioned Low-Reynolds k-ε model of Huang and Coakley was used in order to obtain a better prediction of the Low-Reynolds number turbulent region in the wall vicinity (the coupling between the two models being located at an y^+ of about 30).

The Two-Equation models can be compactly written as

$$\frac{Ds_i}{Dt} = P_{s_i} - D_{s_i} + d_{s_i} \qquad (3.1)$$

where s_i can belong to one out of two possible combinations, i.e., $s_i \in \{k, \varepsilon\}$ or $s_i \in \{k, \omega\}$. On a term by term basis, and referring the reader to the original papers, equation (3.1) can be expanded into:

$$d_{s_i} = \frac{\partial}{\partial x_j}\left[\left(\mu + \frac{\mu_t}{\sigma_{s_i}}\right)\frac{\partial s_i}{\partial x_j}\right]$$

for the diffusion term and

	P	D
k	$-\tau_{ij}\frac{\partial U_i}{\partial x_j}$	ε
ε	$C_{\varepsilon_1}P_k\frac{\varepsilon}{k}$	$C_{\varepsilon_2}\frac{\varepsilon^2}{k}$
ω	$C_{\omega_1}\frac{P_k}{\nu_t}$	$C_{\omega_2}\omega^2$

for the remaining production and destruction terms. The SST model further affects the destruction term, ε, on the k transport equation by a factor of C_μ. The Reynolds Stresses Tensor is, according to the linear Boussinesq hypothesis:

$$\tau_{ij} = \frac{2}{3}k\delta_{ij} - \upsilon_t\left(\frac{\partial U_i}{\partial x_j} - \frac{\partial U_j}{\partial x_i}\right)$$

The eddy viscosity can be expressed as

$$\upsilon_t = C_\mu f_\mu \frac{k^2}{\varepsilon}$$

both in the JL model, where $f_\mu = 1$, and in the HC model, where $f_\mu = \tanh\left(\left(y^+/43\right)^2\right)g$, with $g = \max\left(1, 10.1/\sqrt{Re_t}\right)$. The C_μ constant assumes the usual value of 0.09. In the SST model, Menter implemented a suggestion of Bradshaw, saying that the principal turbulent shear stress, in the wake component of the Boundary Layer, should be made proportional to the local value of the turbulent kinetic energy. Menter therefore proposes:

$$\upsilon_t = \frac{a_1 k}{\max\left(a_1\omega; \Omega F_2\right)}$$

where Ω is the vorticity and F_2 a model function. It's value is

$$F_2 = \tanh\left(arg_2^2\right)$$

$$arg_2 = \max\left(2\frac{\sqrt{k}}{C_\mu\omega y}; \frac{500\nu}{\omega y^2}\right)$$

which uses the normal distance to the wall, y. Furthermore, the SST model solves a combination of a k-ε and a k-ω model, for which he employs a transformed ε equation, written in function of ω. The k-ω model is employed near the wall, whereas the k-ε model is used above this. In this way the traditionally reported sensitivity of the k-ω to the ω freestream values is removed. The blending of the models is done trough a weighting function, F_1, which affects the k-ω model trough it's own value and the k-ε model trough (1- F_1). This last function can be written as

$$F_1 = \tanh\left(arg_1^4\right)$$

$$arg_1 = \min\left[\max\left(2\frac{\sqrt{k}}{C_\mu\omega y}; \frac{500\nu}{\omega y^2}\right); \frac{4\rho}{CD_{k\omega}y^2\sigma_{k_{k-\varepsilon}}}\right]$$

$$CD_{k\omega} = \max\left(2\rho\frac{1}{\sigma_{k_{k-\varepsilon}}\omega}\frac{\partial k}{\partial x_j}\frac{\partial\omega}{\partial x_j}; 10^{-20}\right)$$

The value of the constants, which vary from model to model, are given in the following table:

	σ_k	$\sigma_{\varepsilon/\omega}$	C_{ε_1}	C_{ε_2}	C_{ω_1}	C_{ω_2}
JL	1.	1.3	1.44	1.92	-	-
HC	1.3	1.87	1.5	1.8/g	-	-
SST k-ε	1.	1.17	-	-	0.44	0.0828
SST k-ω	1.18	2.	-	-	0.55	0.075

The boundary conditions for the JL model were given by a law of wall, whereas for the remaining two models the boundary conditions can summarized as follows:

	k	ε/ω
HC	0.	$\frac{2\nu k_p}{(\delta n)^2}$
SST	0.	$7.2\frac{\nu}{(\delta n)^2}$

In this last table, δn is the distance of the first point to the profile's surface and the *p* subscript indicates the value of the variable at this point. For the HC model, the value of ε is imposed at that first point. Moreover, the first point of the mesh and over the profile, is consistently below an y^+ of 1, as required and desired for the application of both the Low-Reynolds model as well as the k-ω model. The boundary condition for ω is the one proposed by Wilcox[15] for his k-ω model.

As for the RST model, the transport equation for the Reynolds stresses is:

$$\frac{D\tau_{ij}}{Dt} = P_{ij} - D_{ij} + d_{ij} + \Phi_{ij}$$

which, for the Gibson and Launder model takes the form:

$$P_{ij} = -\left(\tau_{ik}\frac{\partial U_j}{\partial x_k} + \tau_{jk}\frac{\partial U_i}{\partial x_k}\right)$$

$$D_{ij} = \frac{2}{3}\varepsilon\delta_{ij}$$

$$d_{ij} = \frac{\partial}{\partial x_k}\left(\left(\mu\delta_{kl} + C_s\frac{k\tau_{kl}}{\varepsilon}\right)\frac{\partial\tau_{ij}}{\partial x_l}\right)$$

$$\Phi_{ij} = -C_1\frac{\varepsilon}{k}\left(\tau_{ij} - \frac{2}{3}k\delta_{ij}\right) -$$

$$-C_2\left(P_{ij} - \frac{1}{3}P_{kk}\delta_{ij}\right) + \Phi_{ij}^{wall}$$

$$\Phi_{ij}^{wall} = C_1'\frac{\varepsilon}{k}\left(\tau_{km}n_k n_m\delta_{ij} - \frac{3}{2}\tau_{ik}n_j n_k - \right.$$

$$\left.\frac{3}{2}\tau_{jk}n_i n_k\right)f$$

$$f = \frac{k^{3/2}}{2.5\varepsilon y}$$

$$C_s = 0.22,\ C_1 = 1.8,\ C_2 = 0.6,\ C_1' = 0.5$$

where $\tau_{ij} = \overline{u_i u_j}$, on which the lowercase letters represent fluctuating values. Please note that only one part of the wall reflection terms of the model is retained, on the grounds that, if done otherwise, an excessive level of isotropy would be achieved on the region near to the wall. The ε equation, used in the framework of Second-Order Differential Reynolds Stresses Closure incorporates the Generalized Gradient Diffusion Hypothesis

$$d_\varepsilon = \frac{\partial}{\partial x_k}\left[\left(\mu\delta_{kl} + C_\varepsilon\frac{k\tau_{kl}}{\varepsilon}\right)\frac{\partial\varepsilon}{\partial x_l}\right]$$

with the constants:

$$C_{\varepsilon_1} = 1.44;\ C_{\varepsilon_2} = 1.92;\ C_\varepsilon = 0.18$$

As previously mentioned, on the semi-viscous part of the Boundary Layer, the HC model is solved since the RST model does not comprise any modification to account for this low-Reynolds number region in the flow field. The interface is located at a value of y^+ of about 30 from the wall.

Results

Grid Convergence Index

In order to establish an error bound for the results to be presented, and following a 2σ spirit for the definition and establishment of such a bond, one can follow Roache[16] and his definition of a Grid Convergence Index. Towards it, we possess two grids on which the calculations were performed. The finest of the grids had 352x64 control volumes, whereas the coarsest of grid had 176x32. The coarsest grid corresponds to halving the finest grid on both directions, which yields a GCI for the velocity field of 1.43 % corresponding to the SONIC-Q scheme and RST model. So, results presented with a grid of 352x64 are satisfactory to evaluate the performance of different numerical and turbulence models. The grids are of a C type with a frontier placed at 10 times the chord from the profile's surface.

Influence of Numerical Scheme

To assess the influence of the numerical schemes on the results, one can look at the the flowfield feature that most directly influences the overall results, i.e., the turbulent separated flow region that sets in at the trailing edge. For this one looks at the velocity profiles that, at a 99 percent chord, the turbulence models return for the different numerical discretization schemes.

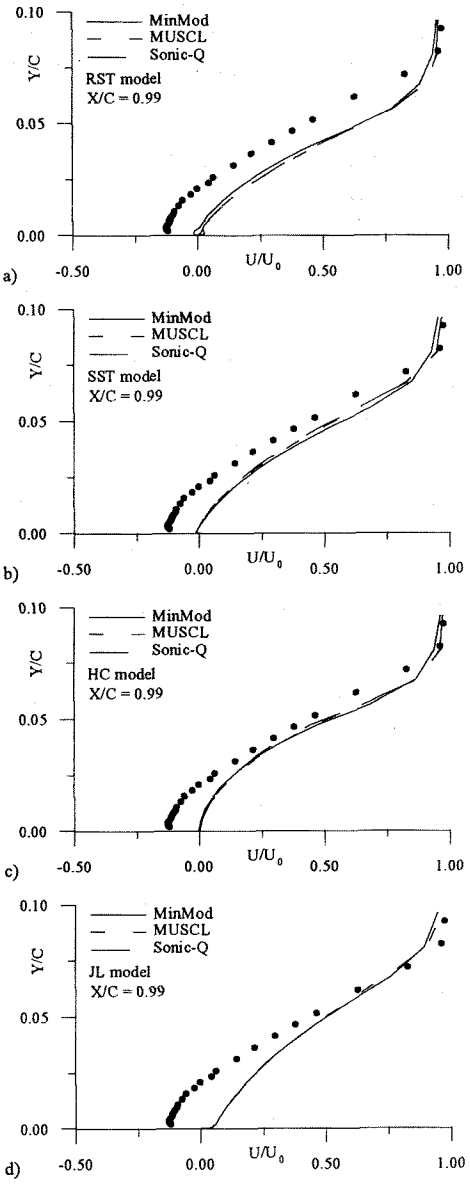

Figure 1 - Velocity plots at X/C = 0.99, α = 13.3°, Ma = 0.15, Re = 2.0×10^6.

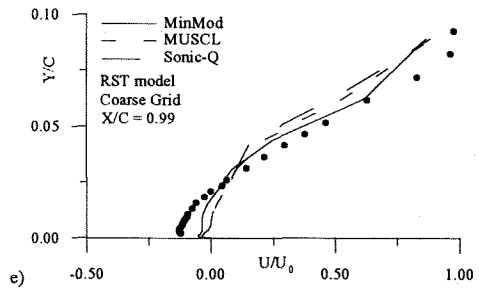

Figure 1 - Velocity plots at X/C = 0.99, α = 13.3°, Ma = 0.15, Re = 2.0x10^6, continuation.

Upon a brief observation that none of the models predicts well the small separated flow region, one may notice that the implication of the numerical scheme is of a two character nature: i) for both the HC and the Jl model, virtually no influence of the numerical discretization scheme is detected, which is in accordance with the Grid Convergence Index results; and ii) for the RST and SST models, the predictions using SONIC-Q, MUSCL and MinMod display a very small difference close to the wall. However, these small differences deserve a detailed analysis because the most accurate schemes (SONIC-Q and MUSCL) do not predict any separation while the less accurate one, MinMod, predicts a small and very thin separated region (see figure 1). One should stress again that the numerical schemes have been used in all transport equations.

Contrary to one expectations, the coarse grid shows a flow separation for all the schemes and a very large one for the MinMod scheme. Comparison of figure 1a) and 1e) show that the turbulence model requires numerical dissipation, given by the less accurate numerical scheme, to give solutions that are closer to the experiments. These results somehow imply that, for this case, some of the limitations of the turbulence model may be improved by less accurate numerical schemes. As a conclusion, better turbulence models are required.

Influence of Turbulence Model

If we now restrain ourselves to the MINMOD scheme, we can look at the influence of the turbulence model in the results. In order to establish such a reasoning, we present the profiles of the variables that most affect the predictions. The section on which they are shown are indicated. We first begin with velocity profiles that show good agreement with the experiments up to X/C = 0.8, see figure 2. The Reynolds stress components (see figure 3) are much better calculated using RST than by SST, HC or JL models.

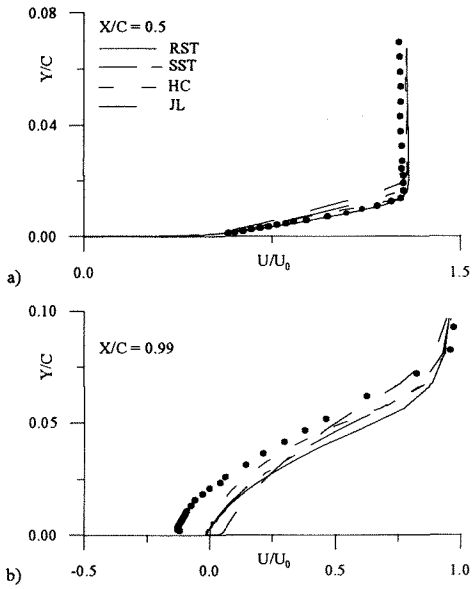

Figure 2 - Velocity profiles.

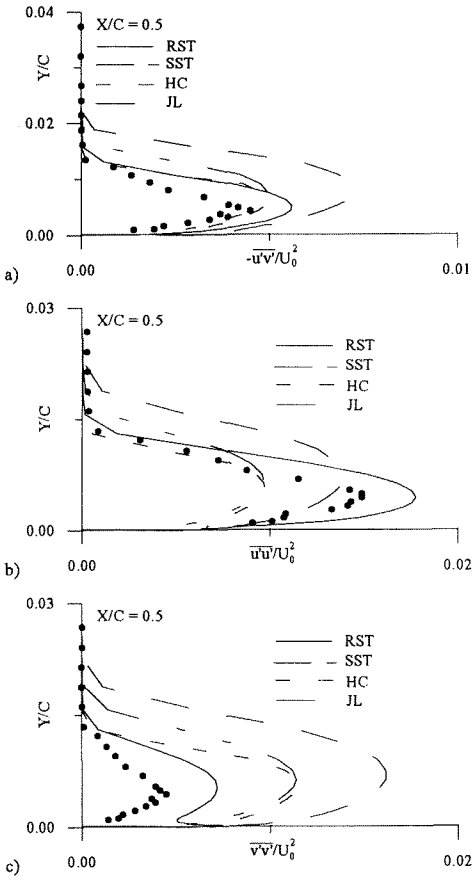

Figure 3 - Reynolds stresses profiles.

The Turbulence anisotropy was well captured by the RST model, although the normal Reynolds stresses denote a kink due to the two layer treatment and the model predicts almost 2k/3 .

Flowfield Summary

Figure 4 comprises the values of C_L and C_D (which are from the aerodynamicist point of view of greatest concern) for all the four models.

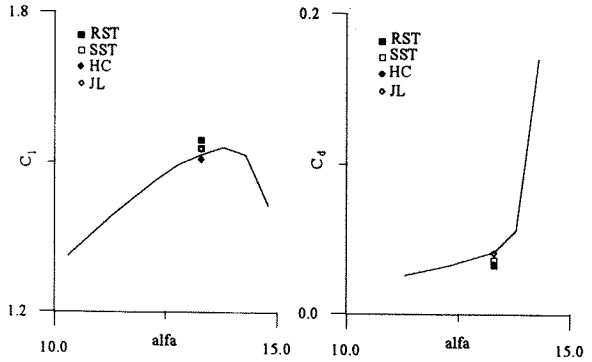

Figure 1 - C_L and C_D plots, $\alpha = 13.3°$, $Ma = 0.15$, $Re = 2.0x10^6$.

One can observe that, for all the models, the results are virtually indistinguishable, what, from an application point of view is a good outcome but, from a modeling point of view, can be a rather disappointing result. If one now wants to understand the reason for such a set of results, one should look at the pressure and velocity fields predictions. This information can be best summarized with a C_p and C_f (module) plot, which follow.

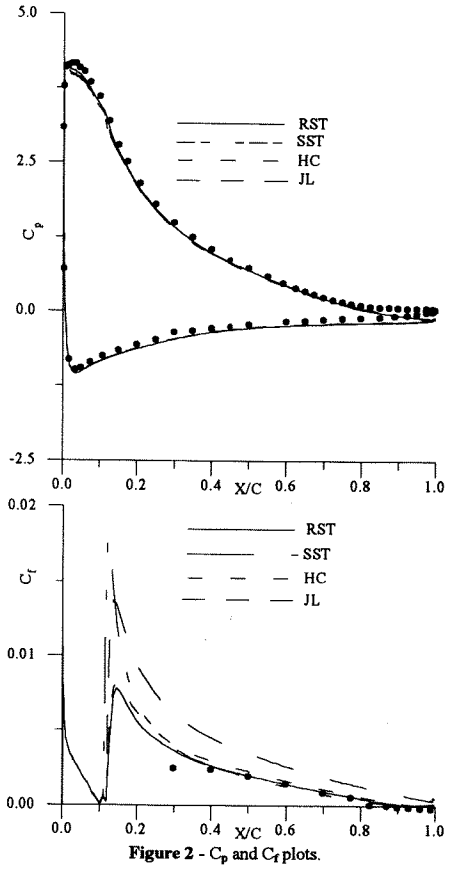

Figure 2 - C_p and C_f plots.

The aerofoil undergoes a leading-edge type of stall, as is easily accepted once this a high-lift aerofoil (measurements for other angles of attack support this conclusion). This means that downstream, near the trailing edge, there is a turbulent separation bubble, that starts in at about 80 percent of chord, as can be seen both from the C_p (in it's region of constant value, "dead air" zone) as well as in the C_f plot. Nevertheless, the fact is that it is the trailing edge separated flow region that controls the accuracy of the predicted values of C_L and C_D. We can see that, for instance, the RST model returns the better prediction for the suction peak, what explains the higher level of C_L, but it fails to capture the trailing edge separation, which explains the overprediction of C_L and the underprediction of C_D. The same reasoning could be applied , *mutatis mutandis*, to explain the results of the other turbulence models. Worth of mention is, however, the extremely high overprediction of the friction coefficient by the Standard k-ε model. This fact is sustained by an overprediction of the turbulence kinetic energy over the entire flowfield and specially near the wall, what was already seen in a previous section. The SST model, on the other hand, immediately after the transition point, also returned an excessive value for the friction coefficient, albeit only in the vicinity of the transition region.

Conclusions

Numerical calculations of the time averaged Navier-Stokes equations were reported for the flow around an high-lift aerofoil at $Re = 2.x10^6$, $Ma = 0.15$ and an angle of attack of 13.3°. A comparison between a large set of predictions obtained using a Reynolds Stress Model, SST, HC and JL models, together with one (SONIC-Q, MUSCL, MinMod) of the three numerical schemes allows the following conclusions:

1. As expected, the pressure coefficient distribution and friction coefficient were well predicted with all turbulence models and numerical schemes up to the separated flow region;
2. Convective discretization influences the turbulence model predictions. In this flow test case, the turbulence model requires additional numerical dissipation, provided by the less accurate numerical scheme MinMod (when compared with MUSCL and SONICQ to retain the best results when compared with experimental velocity data in the separated region vicinity);
3. The k-ε model with wall functions is not appropriate to predict Airfoil stall flows ;
4. The RST model, used together with the HC model in the Low-Reynolds region, satisfactorily predicts the turbulent flow characteristics, specially the turbulence anisotropy;
5. A Low-Reynolds RST model may represent the minimum modeling requirement to predict the mean and turbulence characteristics of Airfoil stall flows.

Further work is currently under way by the authors in this area.

References

[1] Piccin, O. and Cassoudesalle, D. (1987): *"Étude dans la Soufflerie F1 des Profiles AS239 et AS240"*, ONERA Technical Report P.V. 73/1685AYG;

[2] Lien, F.S. and Leschziner, M.A. (1994): *"Modeling 2D Separation from High-Lift Aerofoil with Non-Linear Eddy-Viscosity Model and Second-Moment Closure"*, UMIST Report TFD/95/05;

[3] van Leer, B. (1979) *"Towards the ultimate conservative difference scheme, V. A second order sequel to Godunov's method", J. Comp. Phys.*, 32, p. 101.

[4] Kobayashi, M.H. and Pereira, J.C.F. (1996) *"A Comparison of Second Order Convection Discretization Schemes for Iincompressible Fluid Flow"*, to appear in Comm. Appl. Num. Meth..

[5] Kobayashi, M.H. and Pereira, J.C.F., (1996) *"A Characteristic Based Pressure Correction at All Speeds"*, AIAA Journal, Vol. 34, pp. 272-280.

[6] Sweby, P.K. (1984) *"High resolution schemes using flux limiter for hyperbolic conservation laws", SIAM J. Numer. Anal.* 21, p. 995.

[7] A. Harten and J. Osher, (1987) *"Uniformly high-order accurate non oscillatory schemes I", SIAM J. Numer. Anal.* 24, p. 279.

[8] H.T. Huynh, (1989) *"Second order accurate non oscillatory schemes for scalar conservation laws"*, NASA TM 102010

[9] B.P. Leonard, (1979) *"A stable and accurate convective modeling procedure based on quadratic interpolation", Comput. Methods Appl. Mech. Engng.* 19, p. 59.

[10] Jones, W.P. and Launder, B.E. (1972): *"The Prediction of Laminarization with a Two-Equation Model of Turbulence"*, Int. J. Heat Mass T., Vol. 15, pp. 301-314;

[11] Coakley, T.J. and Huang, P.G. (1992): *"Turbulence Modeling for High Speed Flows"*, AIAA Paper 92-0436, Reno;

[12] Menter, F.R. (1994): *"Two-Equation Eddy-Viscosity Turbulence Models for Engineering Applications"*, AIAA J., Vol. 32, No. 8, pp. 1598-1605;

[13] Gibson, M.M. and Launder, B.E. (1978): *"Ground Effects on Pressure Fluctuations in the Atmospheric Boundary Layer"*, J.F.M., Vol. 86, Pt. 3, pp. 491-511;

[14] Craft, T.J. and Launder, B.E. (1992): *"New Wall-Reflection Model Applied to the Turbulent Impinging Jet"*, AIAA J., Vol. 30, No. 12, pp. 2970-2972;

[15] Wilcox, D.C. (1991): *"A Half Century Historical Review of the k-ω Model"*, AIAA Paper 91-0615, Reno;

[16] Roache, P.J. (1994): *"Perspective: A Method for Uniform Reporting of Grid Refinement Studies"*, ASME J.F.E., Vol. 116, pp. 405-413;